Multiwavelength, Sub-Nanosecond Yb:YAG/Cr^{4+}:YAG/YVO_4 Passively Q-Switched Raman Microchip Laser

Xiao-Lei Wang, Xiao-Jie Wang, and Jun Dong, *Member, IEEE, Senior Member, OSA*

***Abstract*—We have demonstrated a multiwavelength, sub-nanosecond Yb:YAG/Cr^{4+}:YAG/YVO_4 passively Q-switched Raman microchip laser (PQSRML) emitting at 1–1.26 μm. Multiple wavelength Stokes laser radiations at 1123, 1134, 1260 nm and 1079, 1134, 1157, 1260 nm have been obtained at different pump power levels, respectively. The second-order Stokes laser at 1.26 μm increases rapidly with the pump power and becomes the dominant component in the laser emitting spectrum. The maximum average output powerof 135.4 mW is achieved at the absorbed pump power of 2.64 W, meanwhile, the pulse duration is 440 ps, and the peak power is 9.2 kW for the Raman laser. The repetition rate of 20.3 kHz has been achieved. The multi-wavelength, sub-nanosecond lasers at 1–1.26 μm with adjustable frequency separation depending on pump power have potential applications in terahertz wave generation, photodynamic therapy, and generating red laser.**

***Index Terms*—Laser-diode pumped, microchip lasers, passively Q-switched, Raman lasers, Yb:YAG.**

I. Introduction

COMPACT pulsed lasers with simultaneous dual- or multi-wavelength oscillation possess significant practical applications in disease treatment [1], optical sensing [2], holographic interferometry [3], differential absorption laser lidar (DIAL) [4], optical communication [5], and generating terahertz (THz) wave radiation with difference-frequency generation (DFG) method [6]. The pulsed dual- or multi-wavelength solid-state lasers have been obtained by using multiple fluorescent emission lines of Nd^{3+} doped laser materials [7]–[10]. However, extra optical elements such as frequency selector, etalon or specially designed coatings are needed to balance the gain and loss for the individual emission peak line, which makes the laser complicated and high cost. Recently, pulsed dual-wavelength laser has been produced in a resonator with two different laser gain media [11]. The optical parametric oscillator (OPO) is a traditional method for generating multi-wavelength oscillation [12], however, the strict phase matching required in the OPO system introduces instabilities owing to the temperature rising of nonlinear crystals or the misalignment of cavity. Pulsed multi-wavelength lasers have been synchronized with stimulated Raman scattering (SRS) effect and become a hotspot for developing compact multi-wavelength lasers with high peak power. The advantages such as free of phase-matching condition, clean-up effect and cascaded characteristics of SRS make Raman laser an efficient and flexible method to generate new laser radiations, which are difficultly obtained by direct lasing from conventional rare-earth doped laser media. For example, there is a lack of laser gain material with high gain property at 1.1–1.3 μm. It has been demonstrated that the lasers oscillating at 1100–1150 nm are ideal pump sources for directly pumping Ho^{3+}-doped fiber lasers without sensitizers [13] and generating yellow laser by frequency doubling [14]. The laser around 1.26 μm can be used as the laser source to excite oxygen directly in drug-free photodynamic therapy (PDT) for the treatment of some oncological diseases [15], [16]. Moreover, the solid-state red lasers at 630 nm by frequency doubling of 1.26 μm have been identified as simple and robust laser sources replacing the conventional dye red lasers pumped by huge argon or metal vapor lasers for the treatment of nonmelanoma skin cancers (NMSCs) [17], [18]. Therefore, the development of the multi-wavelength Raman lasers at 1–1.3 μm based on the SRS nonlinear process is of great scientific and practical value.

Among various Raman crystals, YVO_4 crystal has been proven to be an excellent Raman crystal with good optical and mechanical properties such as large Raman gain coefficient, high laser damage threshold and a relative broad spectral transparency region. YVO_4 crystals doped with Nd^{3+} or Yb^{3+} ions are also great candidates for self-Raman lasers to reduce the intracavity loss [19]. Moreover, YVO_4 crystal possesses multiple Raman frequency shift lines for generating multi-wavelength Raman laser with small frequency separation. Acoustic-optic (AO) Q-switched, dual- or multi-wavelength intracavity Raman lasers using conventional Nd^{3+} doped laser materials and YVO_4 Raman crystals operating at 1174 nm/1175 nm [20], 1178.9 nm/1199.9 nm [21], 1522 nm/1524 nm [22], and 1.2–1.3 μm [23] have been reported. However, long cavity and active Q-switch make the laser system complex and unsuitable for generating short pulse duration. A miniature, economic,

Manuscript received August 24, 2017; revised December 4, 2017 and January 9, 2018; accepted January 9, 2018. Date of publication January 15, 2018; date of current version February 7, 2018. This work was supported in part by the National Natural Science Foundation of China under Grants 61475130 and 61275143, and in part by the Program for New Century Excellent Talents in University under Grant NCET-09-0669. *(Corresponding author: Jun Dong.)*

The authors are with the Laboratory of Laser and Applied Photonics, Department of Electronics Engineering, Xiamen University, Xiamen 361005, China (e-mail: wangxiaolei@stu.xmu.edu.cn; wangxj@stu.xmu.edu.cn; jdong@xmu.edu.cn).

Color versions of one or more of the figures in this paper are available online at http://ieeexplore.ieee.org.

Digital Object Identifier 10.1109/JSTQE.2018.2792845

1077-260X © 2018 IEEE. Personal use is permitted, but republication/redistribution requires IEEE permission.
See http://www.ieee.org/publications_standards/publications/rights/index.html for more information.

Authorized licensed use limited to: Xiamen University. Downloaded on November 11,2020 at 03:33:03 UTC from IEEE Xplore. Restrictions apply.

multi-wavelength laser with sub-nanosecond pulse duration and high peak power is extremely needed for many applications such as ranging and imaging with high resolution [24], [25], microfabrication, nonlinear frequency conversion, and remote sensing [26], [27]. Passively Q-switched microchip lasers (PQSMLs) have been widely used to generate sub-nanosecond or picosecond pulses due to the extremely short cavity [28], [29]. And PQSMLs are relatively stable, insensitive to misalignment, and suitable for commercially fabricated [28], [30]. Therefore, combining SRS conversion process with LD pumped PQSML is a reasonable solution for developing high peak power, sub-nanosecond pulse duration, multi-wavelength lasers. A sub-nanosecond, Cr^{4+}:YAG passively Q-switched Raman microchip laser (PQSRML) using Nd:LSB or Nd:YAG laser crystal and $Ba(NO_3)_2$ Raman crystal was firstly reported in 2003 [31], which provides a new method for generating short pulses with multiple laser emission.

Compared with Nd^{3+} doped laser crystals, ytterbium (Yb) ions doped laser gain media are more suitable for developing miniature multi-wavelength microchip lasers with high peak power because of their excellent properties such as broad spontaneous emission spectra, simple energy level structure, long fluorescence lifetime, high doping concentration and low thermal loading [32]. PQSMLs with sub-nanosecond pulse duration using Yb:YAG [33] and Yb:$KLu(WO_4)_2$ [34] as laser gain media emitting at 1 μm have been demonstrated. Yb^{3+}:$KGd(WO_4)_2$ [35], [36], Yb^{3+}:$KY(WO_4)_2$ [37], Yb:$KLu(WO_4)_2$ [38], [39] and Yb^{3+}:YVO_4 [40] crystals have been used to generate first-order Stokes laser at 1.1 μm in Cr^{4+}:YAG passively Q-switched lasers. The performance of self-Raman lasers are restricted by the severe thermal loading induced by the simultaneously fundamental laser and Stokes laser oscillating in one crystal. Moreover, the tradeoff between the fundament laser and Raman laser oscillation in self-Raman gain medium makes the self-Raman laser difficult to be optimized and the output laser wavelengths difficult to control. In 2015, an AO Q-switched intracavity Yb:YAG/YVO_4 Raman laser emitting at 1157.6 nm was firstly reported [41]. Recently, a passively Q-switched Raman laser emitting at 1092.6 nm–1290.1 nm using Yb:YAG/YAG/Cr^{4+}:YAG/YAG composite crystal and YVO_4 Raman crystal has been experimentally demonstrated [42]. Composite laser materials are ideal for developing miniature passively Q-switched Raman laser when the doping concentration and thickness of different optical materials are optimized. Therefore, more efforts are extremely needed for developing high peak power, multi-wavelength PQSRMLs with separated laser medium and Raman medium.

In this paper, simultaneous multiple wavelength Raman lines emitting at 1–1.26 μm have been generated from a LD end-pumped PQSRML with a Yb:YAG crystal as gain medium and a YVO_4 crystal as Raman medium. Sub-nanosecond, multi-wavelength laser has been obtained with Raman frequency shift lines of 890 cm^{-1}, 816 cm^{-1}, and 259 cm^{-1} as well as cascaded SRS process of YVO_4 crystal originated from 1030 and 1050 nm fundamental lasers. The pump power dependent Raman laser emitting spectra have been investigated based on the competition among different Raman vibrational modes and different fundamental laser wavelengths. Four Stokes laser lines have been simultaneously obtained as the absorbed pump power (P_{abs}) exceeds 2.17 W. The average output power of 135.4 mW and repetition rate of 20.3 kHz have been achieved at P_{abs} = 2.64 W. The Raman laser with pulse duration of 440 ps and the peak power of 9.2 kW has been obtained in the Yb:YAG/Cr^{4+}:YAG/YVO_4 PQSRML.

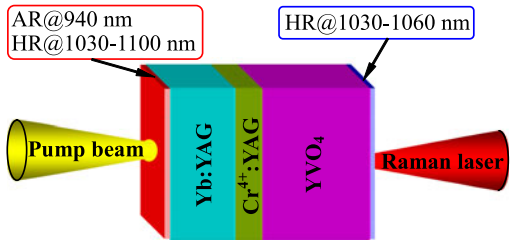

Fig. 1. Schematic diagram for a 940 nm laser-diode end-pumped Yb:YAG/Cr^{4+}:YAG/YVO_4 PQSRML.

II. Experimental Arrangement

The experimental configuration of the LD end-pumped Yb:YAG/Cr^{4+}:YAG/YVO_4 PQSRML for generating multi-wavelength laser radiation is shown in Fig. 1. A continuous-wave, fiber-coupled 940 nm LD arrays with a fiber core size of 200 μm and numerical aperture (N.A.) of 0.22 was served as the pump source. The optical coupling system was a combination of two aspheric lenses with 8 mm focal length. The incident pump beam was re-imaged inside the Yb:YAG crystal with a focused spot diameter of about 100 μm. A 1.2-mm-thick, 10 at.% doped Yb:YAG crystal and a 2-mm thick, c-cut YVO_4 crystal were selected as the laser gain crystal and Raman conversion crystal, respectively. The rear mirror of the microchip laser was formed by directly coating in the rear surface of the Yb:YAG crystal with anti-reflection (AR) at 940 nm and high-reflected (HR) at 1030 nm–1100 nm (R > 99.8%). The intracavity surfaces of the Yb:YAG and YVO_4 crystals were AR coated at 1030 nm–1100 nm to decline the internal loss. The output coupler (OC) of the microchip laser was formed with one surface of YVO_4 crystal coated with T $\approx$ 1% at 1030 nm, T < 0.5% at 1040–1140 nm, T $\approx$ 1.5% at 1156 nm and T $\approx$ 29% at 1260 nm, respectively. A 0.5-mm-thick Cr^{4+}:YAG crystal with an initial transmission of 95% for 1030 nm was served as a Q-switch, and both surfaces of the Cr^{4+}:YAG crystal were AR coated for minimizing the Fresnel loss. The Cr^{4+}:YAG sample was tightly sandwiched between the Yb:YAG crystal and YVO_4 crystal. The optical elements (Yb:YAG, Cr^{4+}:YAG, and YVO_4 crystal) were mechanically put in contact with each other by two copper holders with 3 mm diameter central apertures, which also act as the heat sink to relieve the thermal accumulation. The overall length of the plane-parallel cavity is only 3.7 mm. The experiments were carried out at room temperature and no active cooler were applied. The average output power was measured by a Thorlabs PM200 power meter in the experiment. An Anritsu optical spectral analyzer (MS9740A) was employed to record the emitting laser spectra. A digital oscilloscope (6 GHz bandwidth, TDS6604, Tektronix Inc.) and a 5 GHz In-

Authorized licensed use limited to: Xiamen University. Downloaded on November 11,2020 at 03:33:03 UTC from IEEE Xplore. Restrictions apply.

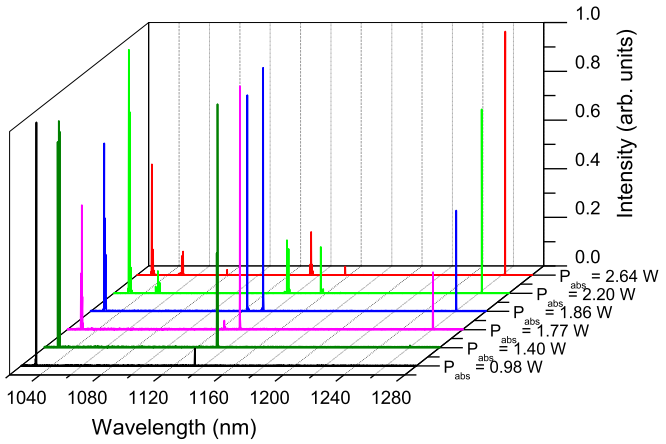

Fig. 2. Evolution of the laser emitting spectra of Yb:YAG/Cr^{4+}:YAG/YVO$_4$ PQSRML at different P$_{abs}$.

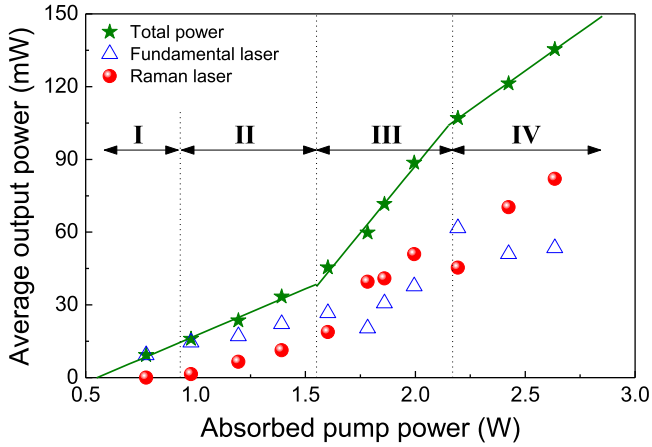

Fig. 3. Average output power of Yb:YAG/Cr^{4+}:YAG/YVO$_4$ PQSRML versus P$_{abs}$. The average output powers of the Raman laser and residual fundamental laser are also plotted at different P$_{abs}$.

GaAs photo-diode were used to record and analysis the laser pulse characteristics.

III. Experimental Results

The absorbed pump powers (P$_{abs}$) of the Yb:YAG crystal in the Yb:YAG/Cr^{4+}:YAG/YVO$_4$ PQSRML at different incident pump powers were obtained by measuring the pump power before incident on the Yb:YAG crystal and after passing through the Yb:YAG crystal. The absorption efficiency of the Yb:YAG crystal at different incident pump powers was around 62%. Fig. 2 depicts the evolution of the lasing spectra of the Yb:YAG/Cr^{4+}:YAG/YVO$_4$ PQSRML at different P$_{abs}$. The wavelengths of the Stokes laser and the residual fundamental laser were shown in the laser emitting spectra. The Raman laser at 1134.24 nm is the first-order Stokes laser with the strongest Raman frequency shift of 890 cm^{-1} converted from 1030 nm fundamental laser when P$_{abs}$ reaches the Raman lasing threshold of approximately 0.93 W. With further increase in P$_{abs}$, the intensity of the first-order Stokes laser at 1134 nm increases continuously. When P$_{abs}$ reaches 1.4 W, the intensity of the first-order Stokes laser is nearly the same as that of the 1030 nm fundamental laser. As P$_{abs}$ was further increased to over 1.55 W, two new Raman laser radiations at 1123.04 nm and 1260.52 nm were generated, which were the first-order Stokes laser with the Raman shift of 816 cm^{-1} and the second-order Stokes laser with the Raman shift of 890 cm^{-1}, respectively. The Raman laser simultaneously oscillated at 1123.04 nm, 1134.24 nm, and 1260.52 nm, while the fundamental laser still oscillated at 1030 nm at P$_{abs}$ = 1.77 W. The second-order Stokes laser at 1260 nm is attributed to the sufficient intracavity intensity of the first-order Stokes laser at 1134 nm, which served as the pump source for the second-order Stokes laser. Multi-wavelength oscillation around 1030 nm, 1123 nm, 1134 nm, and 1260 nm is kept when P$_{abs}$ is within the range between 1.55 W and 2.17 W. When P$_{abs}$ is increased to 2.2 W, the first-order Stokes laser at 1123 nm disappears, while a new fundamental laser at 1050 nm and a new Raman laser at 1156.22 nm begin to oscillate. The new Raman laser at 1156 nm is the first-order Stokes laser with the Raman shift of 890 cm^{-1} converted from the 1050 nm fundamental laser. The second-order Stokes laser increases rapidly and becomes the major component in the laser emitting spectrum when P$_{abs}$ exceeds 1.86 W. When P$_{abs}$ was further increased to 2.64 W, a weak first-order Stokes laser at 1079.22 nm converted from the 1050 nm fundamental laser with the Raman shift of 259 cm^{-1} was observed. The intensities of the first-order Stokes lasers at 1134 nm and 1156 nm as well as the fundamental laser at 1030 nm and 1050 nm gradually decrease, and the intensity of the second-order Stokes laser at 1260 nm becomes stronger with P$_{abs}$ when P$_{abs}$ exceeds 2.17 W. The laser spectra at different absorbed pump powers show that fundamental laser, first-order Stokes laser and second-order Stokes laser shift to longer wavelength (red-shift) with the absorbed pump power. However, the relative intensities of multiple laser lines maintained stable over time when the pump power was set.

Fig. 3 shows the variation of the average output power of the Yb:YAG/Cr^{4+}:YAG/YVO$_4$ PQSRML as a function of P$_{abs}$. A longpass filter was employed to split the Raman laser and fundamental laser. The measured average output powers of the fundamental laser and Raman laser at different P$_{abs}$ are also shown in Fig. 3. The 1030 nm fundamental lasing threshold was about 0.74 W. The 1134 nm Raman laser started to oscillate when P$_{abs}$ was increased to approximately 0.93 W. When the intracavity peak power intensity exceeds the SRS threshold, the simultaneous multiple Stokes lasers operation in the Yb:YAG/Cr^{4+}:YAG/YVO$_4$ PQSRML is dominant, and has significant impact on the average output power. The total average output power does not increase linearly with P$_{abs}$. Based on the laser oscillating wavelength (as shown in Fig. 2), the variation of the output power with P$_{abs}$ can be divided into four sections, as shown in Fig. 3. The total average output power of 1030 nm fundamental laser and 1134 nm Raman laser increases linearly with P$_{abs}$ when P$_{abs}$ is lower than 1.55 W. The slope efficiency is 4.7%. When P$_{abs}$ is within the range between 1.55 W and 2.17 W, 1123 nm Raman laser and 1260 nm second-order Stokes laser together with 1030 nm fundamental laser and 1134 nm Raman laser oscillate simultaneously. The total average output power increases fast with P$_{abs}$, and the slope efficiency is increased

Authorized licensed use limited to: Xiamen University. Downloaded on November 11,2020 at 03:33:03 UTC from IEEE Xplore. Restrictions apply.

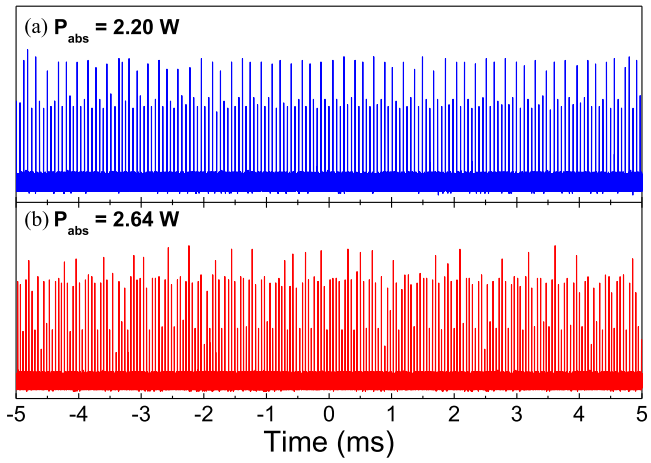

Fig. 4. Typical pulse trains of Yb:YAG/Cr^{4+}:YAG/YVO_4 PQSRML at P_{abs} = 2.2 W and 2.64 W, respectively.

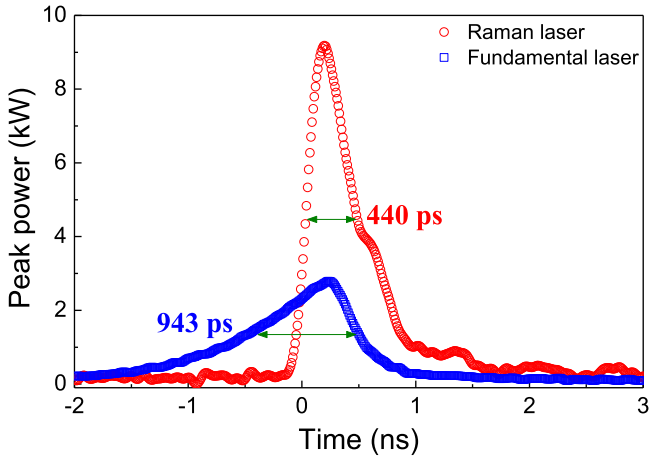

Fig. 5. Typical fundamental laser pulse profile and Raman laser pulse profile in the Yb:YAG/Cr^{4+}:YAG/YVO_4 PQSRML at P_{abs} = 2.64 W.

to 11%. When P_{abs} is higher than 2.17 W, the Raman laser converted from 1030 nm and 1050 nm dual-wavelength fundamental laser intensifies the competition among the Raman lasers. The total average output power increases linearly with P_{abs}, however, the slope efficiency is decreased to 6.4%. The decline of the slope efficiency at the high pump power was due to the strong gain competitions among different fundamental lasers as well as Raman lasers. And severe thermal loading under high pump powers leads to the decease of Raman gain coefficient [43], which is also a reason for drop of the slope efficiency. The average output power was 135.4 mW and the optical-to-optical efficiency was 5.2% at P_{abs} = 2.64 W. The output power of the Yb:YAG/Cr^{4+}:YAG/YVO_4 PQSRML can be further scaled up by utilizing longer Raman crystal and optimizing the coating parameters of both the laser crystal and Raman crystal. Another alternative approach to enhance performance of PQSRML is applying thermal bonding technique to decline the intracavity loss with less number of optical surfaces in the future. The output Raman laser beam profiles were monitored and measured at different absorbed pump powers. The transverse laser profiles are nearly TEM_{00} mode and the measured beam quality factor M^2 is less than 1.3 which shows a near-diffraction-limited beam quality achieved in the Yb:YAG/Cr^{4+}:YAG/YVO_4 PQSRML. The intracavity laser mode size was estimated to be 80 μm in diameter by measuring the output beam diameter near the output coupler.

Because the Raman laser in the Yb:YAG/Cr^{4+}:YAG/YVO_4 PQSRML is converted from the intracavity fundamental laser through SRS nonlinear process, the output pulse trains of the Raman laser is synchronized with that of the fundamental laser. Therefore, the repetition rate is identical for the Raman laser and the fundamental laser when P_{abs} is above the Raman laser threshold. Fig. 4 depicts the typical pulse trains in the Yb:YAG/Cr^{4+}:YAG/YVO_4 PQSRML at P_{abs} = 2.2 W and 2.64 W, respectively. The periodical pulsation was observed in the pulse trains at different P_{abs}. The periodical pulsation in the Yb:YAG/Cr^{4+}:YAG/YVO_4 PQSRML is caused by the multi-longitudinal mode oscillation of the fundamental laser around 1030 nm and 1050 nm. The multi-longitudinal mode oscillation induced periodical pulsation has been observed in the Cr^{4+}:YAG passively Q-switched Yb:YAG microchip laser [44]. The longitudinal modes induced periodical pulsation in passively Q-switched Yb:YAG microchip laser can be alleviated by adjusting the intensities and mode separation among the longitudinal modes through tilting etalon effect. The separation and intensities of the longitudinal modes can be controlled by adjusting the thickness of Yb:YAG, Cr^{4+}:YAG and YVO_4 crystals in Yb:YAG/Cr^{4+}:YAG/YVO_4 PQSRML. Therefore, the stable pulse trains with relative small amplitude fluctuation is expected for potential applications in the Yb:YAG/Cr^{4+}:YAG/YVO_4 PQSRML.

The output pulse profiles of the fundamental laser and Raman laser were measured by separating the fundamental laser and Raman laser at different absorbed pump powers. The measured pulse profiles of the residual fundamental laser and the Raman laser at P_{abs} = 2.64 W are shown in Fig. 5. The Raman laser pulse profile is totally different from the residual fundamental laser pulse profile. The Raman laser pulse profile is asymmetrical with sharp rising edge and wide pulse falling edge, while the fundamental laser pulse profile is also asymmetrical with a smooth rising edge and a rapid falling edge. The sharp rising edge in the Raman laser pulse was due to pulse energy extraction from the intracavity fundamental laser pulse and the pulse compression effect of SRS process. Formation of the Raman laser pulse starts from the intracavity fundamental laser pulse rising edge with intensity higher than the Raman laser threshold. And then the Raman laser pulse grows rapidly with rapid depleting fundamental laser field. Therefore, the sharp rising edge in the Raman laser is formed. The measured residual fundamental laser pulse is the remained intracavity fundamental pulse after the extraction of the Raman laser pulse. Thus, the residual fundamental laser pulse exhibits smooth rising edge and sharp fall edge. The Raman laser pulse duration was measured to be 440 ps while the fundamental laser pulse duration was measured to be 943 ps at P_{abs} = 2.64 W. Although the measured Raman laser pulse profile is the overlapping of the Raman laser

Authorized licensed use limited to: Xiamen University. Downloaded on November 11,2020 at 03:33:03 UTC from IEEE Xplore. Restrictions apply.

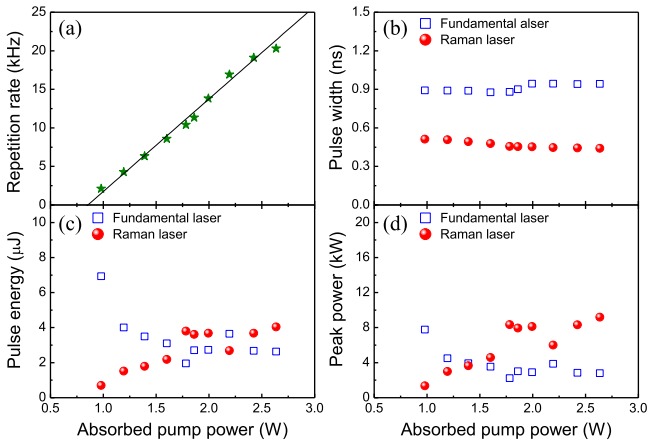

Fig. 6. (a) Repetition rate, (b) pulse width, (c) pulse energy and (d) peak power of the Yb:YAG/Cr^{4+}:YAG/YVO$_4$ PQSRML vs. the absorbed pump power.

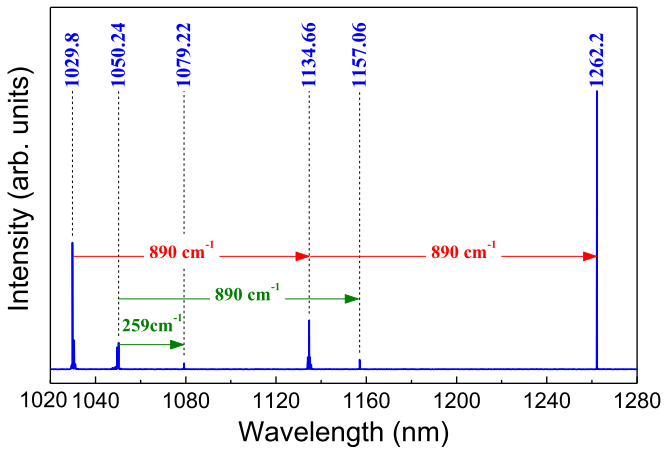

Fig. 7. Raman laser conversion process in Yb:YAG/Cr^{4+}:YAG/YVO$_4$ PQSRML with 1030 nm and 1050 nm dual-wavelength fundamental laser oscillation.

pulses at different wavelengths of 1079.22, 1134.66, 1157.06 and 1262.2 nm (as shown in Fig. 2), the contribution of the 1079.22 nm and 1157.06 nm Raman laser can be neglected. Therefore, the measured Raman laser pulse is the overlap of the pulses of 1134.66 nm and 1262.2 nm, the 1262.2 nm Raman laser pulse is the dominant component and is stronger than that of 1134.66 nm owing to the efficient conversion of the first-order Stokes laser to the second-order Stoke laser. Thus, the measured Raman laser pulse profile can be roughly treated as the pulse profile of 1262.2 nm second-order Stokes laser pulse. The theoretical estimation of the Raman laser pulse was done by applying the theoretical formula [45] taking into account the losses of first-order and second-order Stokes laser in Yb:YAG/Cr^{4+}:YAG/YVO$_4$ PQSRML. The theoretically calculated pulse duration is 400 ps, which is in good agreement with the measured Raman laser pulse duration. The pulse duration of Raman laser was dramatically compressed compared to the residual fundamental laser pulse duration. The fundamental laser pulse energy and the Raman laser pulse energy were measured to be 2.63 μJ and 4.04 μJ, respectively. The corresponding peak power of the fundamental laser and Raman laser were 2.8 kW and 9.2 kW, respectively. This peak power is higher than those of the reported self-Raman microchip lasers based on Yb^{3+} doped materials [35], [37], [39], [40], which is benefiting from the good thermal management with separated laser medium and Raman medium configuration.

Fig. 6 shows the repetition rate, pulse width, pulse energy, and peak power of the Yb:YAG/Cr^{4+}:YAG/YVO$_4$ PQSRML varying with the absorbed pump power. The repetition rate of the Yb:YAG/Cr^{4+}:YAG/YVO$_4$ PQSRML increases linearly with P_{abs}. The highest repetition rate is 20.3 kHz at $P_{abs} = 2.64$ W. The fundamental laser pulse duration slightly increases from 900 ps to 943 ps with the increase of P_{abs} from 0.98 W to 2.64 W. While the Raman laser pulse duration decreases from 512 ps to 440 ps as P_{abs} increases from 0.98 W to 2.64 W. The slight broadening of the fundamental laser pulse duration is due to the severe thermal loading under high pump power. For Cr^{4+}:YAG crystal, the initial transmission tends to slightly increase with the rising of temperature [46], which leads to the enlargement of the pulse duration. The fundamental laser pulse energy decreases from 7 μJ to 2.6 μJ and the Raman laser pulse energy increases from 0.7 μJ to 4.04 μJ when P_{abs} increases from 0.98 W to 2.64 W. The peak power of the fundamental laser decreases from 7.76 kW to 2.8 kW, and the peak power of the Raman laser raises from 1.35 kW to 9.2 kW when P_{abs} is increased from 0.98 W to 2.64 W.

IV. Discussions

The multiple wavelengths Raman laser conversion process in Yb:YAG/Cr^{4+}:YAG/YVO$_4$ PQSRML under 1030 and 1050 nm dual-wavelength fundamental laser oscillation is illustrated in Fig. 7 by taking an typical example of the laser emitting spectrum at $P_{abs} = 2.64$ W. 1030 and 1050 nm dual-wavelength fundamental lasers in Yb:YAG/Cr^{4+}:YAG/YVO$_4$ PQSRML make the multi-wavelength Raman laser oscillation more colorful. The Raman laser at 1134 nm is the first-order Stokes laser converted from 1030 nm fundamental laser with Raman shift of 890 cm^{-1} for c-cut YVO$_4$ crystal. The Raman laser at 1262 nm is the second-order Stokes laser converted from the first-order Stokes laser at 1134 nm with Raman shift of 890 cm^{-1}. The first-order Stokes lasers at 1079 nm and 1156 nm are generated with the Raman shift 259 cm^{-1} and 890 cm^{-1} from 1050 nm fundamental laser. The intensities of the multi-wavelength Stokes lasers at 1079 nm, 1134 nm, 1156 nm and 1262 nm are determined by the absorbed pump power and reflection coatings on the YVO$_4$ crystal.

The multi-wavelength Raman laser oscillation in the Yb:YAG/Cr^{4+}:YAG/YVO$_4$ PQSRML is governed by the 1030 nm and 1050 nm dual fundamental laser oscillation of Yb:YAG crystal and the multiple Raman frequency shift lines of YVO$_4$ crystal. When the single-pass gain for the Raman laser is high enough to overcome the losses, the first-order Stokes laser starts to oscillate. The SRS threshold can be described as [47]:

$$R_{in} R_{out} (1 - L) \exp(2 g_R I_{th} l_R) \geq 1 \quad (1)$$

Authorized licensed use limited to: Xiamen University. Downloaded on November 11,2020 at 03:33:03 UTC from IEEE Xplore. Restrictions apply.

where I_{th} is the SRS threshold intensity for the fundamental laser, g_R is the steady-state Raman gain coefficient, l_R is the length of Raman crystal, L is the resonator loss for the Stokes laser, R_{in} is the reflectivity of the rear cavity mirror, and R_{out} is the reflectivity of the OC at the Raman laser wavelength. According to the steady-state Raman gain coefficients of 890 and 816 cm^{-1} of YVO_4 crystal for 1064 nm fundamental laser [19], g_R for 890 cm^{-1} is approximately 1.7 times of that for 816 cm^{-1}. The SRS threshold intensities of the first-order Stokes laser at 1123 nm was calculated to be 1.7 times of that at 1134 nm before the second-order Stokes laser at 1260 nm was generated. The threshold intensity for 1134 nm was lower than that for 1123 nm, so that the first-order Stokes laser at 1134 nm began to oscillate firstly. When the intracavity intensity of the Raman laser at 1134 nm was increased sufficient to overcome the oscillating threshold of the second-order Stokes laser at 1260 nm, the second-order Stokes laser started to oscillate. The conversion from 1134 nm Raman laser to second-order Stokes laser by cascaded SRS effect can be regard as output coupling loss for the first-order Stokes laser. Therefore, the generation of the second-order Stokes laser increases the intracavity single-pass transmission losses of the 1134 nm Raman laser. As the reflection of the YVO_4 crystal at 1134 nm and 1123 nm is nearly the same, the increased loss for 1134 nm Raman laser owing to conversion to 1260 nm second-order Stokes laser makes 1123 nm Raman laser with 816 cm^{-1} Raman shift possible to oscillate. When the intracavity intensity of the 1030 nm fundamental laser was sufficient to overcome the lasing threshold of 1123 nm Raman laser with the Raman vibrational mode line of 816 cm^{-1}, the dual-wavelength Raman laser at 1134 nm and 1123 nm was generated. Meanwhile, two Raman vibrational mode lines compete with each other because they consume the same fundamental laser field. The dual-wavelength fundamental laser operation were mainly due to the gain and loss balance at 1030 nm and 1050 nm induced by aggravated self-absorption at 1030 nm induced by the temperature rising with the increased pump power [32]. Moreover, the nonlinear conversion process of SRS can be treated as a consumption process for the fundamental laser field at the primary emission line of 1030 nm, resulting in the increase of the transmission losses for 1030 nm fundamental laser, which also contributed to the dual-wavelength fundamental laser operation.

The red-shift of the laser wavelength with the pump power in the Yb:YAG/Cr^{4+}:YAG/YVO_4 PQSRML is attributed to the local temperature rise inside Yb:YAG and YVO_4 crystal with increase in the pump power. Temperature rising inside the Yb:YAG crystal and YVO_4 crystal has two effects on the laser emitting wavelengths. The thermal induced expansion of YVO_4 crystal lattice makes the temperature dependent Raman frequency shift with a ratio of -0.023 cm^{-1}/K [43]. While the temperature dependent emission peak of Yb:YAG crystal red-shift with a ratio of 0.008 nm/K [32]. Therefore, the wavelength shift of the second-order Stokes laser in the Yb:YAG/Cr^{4+}:YAG/YVO_4 PQSRML is calculated to be 2.1 nm when the absorbed pump power is increased from 1.7 W to 2.7 W. The calculated wavelength shift with the pump power is in good agreement with the experimental data (1.72 nm red-shift of the second-order Stokes laser as shown in Fig. 2).

TABLE I
COMPARISON OF OUTPUT CHARACTERISTICS OF Cr^{4+}:YAG PASSIVELY Q-SWITCHED Yb^{3+} DOPED CRYSTALS MINIATURE RAMAN LASERS

Crystal	λ_S, nm	P_S, mW	E_s, μJ	P_{peak}, kW	τ_S, ns	Ref.
Yb:YAG/ YVO_4	1079–1260	82	4.04	9.2	0.44	This work
Yb:KLuW	1151	119	3	1.5	2	[39]
Yb:YVO_4	1119.5	89	3.6	0.59	6	[40]
Yb:KGW	1145	110	8.2	11	0.7	[36]
Yb:KGW	1139	7	0.4	0.02	20	[35]

Notes: λ_S –Stokes laser emission wavelength; P_S – maximum average output power of Stokes laser; E_s – maximum pulse energy of Stokes laser; P_{peak} – maximum peak power of Stokes laser; τ_S – shortest pulse width of Stokes laser.

The laser emission results (as shown in Fig. 2) indicate that the efficiency of cascaded SRS converting process is enhanced with P_{abs}. The emerging of 1079 nm, 1123 nm, and 1156 nm can be regarded as parasitic losses and should be avoided to boost the conversion efficiency in the process of cascaded Stokes generation. Therefore, it needs complicated design of mirror coatings or inserting frequency selector in order to increase the oscillation threshold of unwanted Stokes lines. Based on the present microchip laser cavity design, the weak Stokes lines were nearly all suppressed under high pump power. And experimental laser emitting spectral results show that the multiple Stokes lines oscillation has less impact on the generation of second-order Stokes laser in the experiment. Moreover, the multiple Stokes laser oscillation has some special applications in many fields such as terahertz wave generation and visible laser generation with frequency doubling technique. Based on the dual-wavelength oscillation with narrow separation at 1030 nm/1050 nm, 1123 nm/1134 nm, and 1134 nm/1156 nm, the corresponding THz wave frequency of 5.55 THz, 2.59 THz and 5.03 THz can be expected. Combining with SHG (second harmonic generation) or SFG (sum-frequency generation), broadband visible lines ranging from green to red region (515 nm–630 nm) can be produced. These visible radiations have some significant applications in biomedicine, laser display, and optical sensing.

Table I summarizes output laser characteristics of this work and some typical passively Q-switched intracavity miniature Raman lasers with Yb^{3+} ions doped laser crystals as gain media. Besides the shortest pulse width of 440 ps has been achieved in Yb:YAG/Cr^{4+}:YAG/YVO_4 PQSRML, multiple wavelengths of fundamental laser, first-order Stokes laser and second-order Stokes laser have been obtained. The multi-wavelength, sub-nanosecond laser pulses generated in the Yb:YAG/Cr^{4+}:YAG/YVO_4 PQSRML offer a potential laser source for flexible applications comparing to those reported results. The efficient generation of second-order Stokes laser at 1260 nm (about 60% efficiency from the first-order Stokes laser to second-order Stokes laser) under current laser design shows that an effective method for developing efficient cascaded SRS lasers by optimizing the laser components. The output power of

Authorized licensed use limited to: Xiamen University. Downloaded on November 11,2020 at 03:33:03 UTC from IEEE Xplore. Restrictions apply.

the Yb:YAG/Cr^{4+}:YAG/YVO_4 PQSRML can be further scaled up by utilizing longer Raman crystal and optimizing the coating parameters of both the laser crystal and Raman crystal. Moreover, pump power dependent multi-wavelength laser oscillation in the Yb:YAG/Cr^{4+}:YAG/YVO_4 PQSRML provides potential possibilities to develop simultaneous multiple or single specific wavelength laser by optimizing the length and coating parameters of crystals to control the gain and loss for different laser radiations in the PQSRML. Note that the available coating parameters of both the laser crystal and Raman crystal were not optimal for the cascaded SRS generation process. Part of backward-propagating second-order Stokes laser leaked through the input surface of Yb:YAG crystal because of the input surface of Yb:YAG crystal was only HR coated at 1030–1100 nm or were absorbed by Cr^{4+}:YAG crystal. So the performance of the 1262 nm Raman laser generated in the Yb:YAG/Cr^{4+}:YAG/YVO_4 PQSRML could be enhanced with longer length of Raman crystal and higher reflection coating at the wavelengths for both fundamental laser and first-order Stokes laser. Otherwise, high transmission at the wavelength of the second-order Stokes laser as well as appropriate partial transmission at the first-order Stokes laser should be benefit for the efficient performance of the first-order Stokes laser by fully suppressing the oscillation of the second-order Stokes laser.

V. Conclusion

In conclusion, multi-wavelength laser at 1–1.26 μm with sub-nanosecond pulse duration and high repetition rate from a laser-diode end-pumped Yb:YAG/Cr^{4+}:YAG/YVO_4 PQSRML has been demonstrated for the first time to our best knowledge. Simultaneous multi-wavelength Raman lasers at 1123, 1134, and 1260 nm converted from 1030 nm fundamental laser have been achieved under P_{abs} between 1.55 W and 2.17 W in the cascaded SRS generation process. By simultaneously utilizing 1030 nm and 1050 nm fundamental lasers, multi-wavelength Stokes lasers at 1079 nm, 1134 nm, 1156 nm, and 1262 nm have been obtained at $P_{abs} > 2.17$ W. The maximum average output power was measured to be 135.4 mW at $P_{abs} = 2.64$ W. The Raman laser pulse duration of 440 ps, peak power of 9.2 kW, and the repetition rate of 20.3 kHz were achieved at $P_{abs} = 2.64$ W. The high peak power, dual-wavelength laser radiation at 1030 nm/1050 nm, 1123 nm/1134 nm, and 1134 nm/1156 nm paves a new way for developing miniature laser source for laser spectroscopy, pumping Ho^{3+}-doped fiber lasers, generating yellow laser by second harmonic generation and terahertz generation. The high peak power Raman laser around 1260 nm could be a potential laser source in drug-free photodynamic therapy and generating red laser.

References

[1] S. N. Son, J.-J. Song, J. U. Kang, and C.-S. Kim, "Simultaneous second harmonic generation of multiple wavelength laser outputs for medical sensing," *Sensors*, vol. 11, no. 6, pp. 6125–6130, Jun. 2011.

[2] Y. He and B. J. Orr, "Rapidly swept, continuous-wave cavity ring-down spectroscopy with optical heterodyne detection: Single- and multi-wavelength sensing of gases," *Appl. Phys. B, Lasers Opt.*, vol. 75, no. 2, pp. 267–280, Sep. 2002.

[3] F. Weigi, "A generalized technique of two-wavelength, nondiffuse holographic interferometry," *Appl. Opt.*, vol. 10, no. 1, pp. 187–192, Jan. 1971.

[4] M. Wirth *et al.*, "The airborne multi-wavelength water vapor differential absorption lidar WALES: System design and performance," *Appl. Phys. B, Lasers Opt.*, vol. 96, no. 1, pp. 201–213, Feb. 2009.

[5] T. Healy, F. C. Garcia Gunning, A. D. Ellis, and J. D. Bull, "Multi-wavelength source using low drive-voltage amplitude modulators for optical communications," *Opt. Express*, vol. 15, no. 6, pp. 2981–2986, Mar. 2007.

[6] K. Zhong *et al.*, "Efficient continuous-wave 1053-nm Nd:GYSGG laser with passively Q-switched dual-wavelength operation for terahertz generation," *IEEE J. Quantum Electron.*, vol. 49, no. 3, pp. 375–379, Mar. 2013.

[7] H. T. Huang *et al.*, "Intermittent oscillation of 1064 nm and 1342 nm obtained in a diode-pumped doubly passively Q-switched Nd:YVO_4 laser," *Appl. Phys. B, Lasers Opt.*, vol. 96, no. 4, pp. 815–820, Sep. 2009.

[8] L. Guo *et al.*, "1319 nm and 1338 nm dual-wavelength operation of LD end-pumped Nd:YAG ceramic laser," *Opt. Express*, vol. 18, no. 9, pp. 9098–9106, Apr. 2010.

[9] J.-L. Xu *et al.*, "Dual-wavelength oscillation at 1064 and 1342 nm in a passively Q-switched Nd:YVO_4 laser with V^{3+}:YAG as saturable absorber," *Appl. Phys. B, Lasers Opt.*, vol. 103, no. 1, pp. 75–82, Apr. 2011.

[10] K.-G. Hong and M.-D. Wei, "Simultaneous dual-wavelength pulses achieved by mixing spiking and passive Q-switching in a pulsed Nd:$GdVO_4$ laser with a Cr^{4+}:YAG saturable absorber," *Opt. Lett.*, vol. 41, no. 10, pp. 2153–2156, May 2016.

[11] Y.-J. Huang, H.-H. Cho, K.-W. Su, and Y.-F. Chen, "Observation of repetition rate locking in an orthogonally-polarized dual-wavelength passively Q-switched hybrid Nd:YVO_4/Nd:YLF laser," in *Proc. Conf. Lasers Electro-Opt.*, San Jose, CA, USA, 2016, Paper SM3M.6.

[12] H. Chu *et al.*, "Dual-wavelength Nd:LGGG laser intracavity pumped simultaneous OPO and SRS processes in single KTP," *Appl. Opt.*, vol. 55, no. 8, pp. 1824–1829, Mar. 2016.

[13] S. D. Jackson, F. Bugge, and G. Erbert, "Directly diode-pumped holmium fiber lasers," *Opt. Lett.*, vol. 32, no. 17, pp. 2496–2498, Sep. 2007.

[14] H. M. Pask, "The design and operation of solid-state Raman lasers," *Prog. Quantum Electron.*, vol. 27, no. 1, pp. 3–56, Jan. 2003.

[15] A. S. Yusupov, S. E. Goncharov, I. D. Zalevskii, V. M. Paramonov, and A. S. Kurkov, "Raman fiber laser for the drug-free photodynamic therapy," *Laser Phys.*, vol. 20, no. 2, pp. 357–359, Feb. 2010.

[16] F. Anquez, E. Courtade, A. Sivéry, P. Suret, and S. Randoux, "A high-power tunable Raman fiber ring laser for the investigation of singlet oxygen production from direct laser excitation around 1270 nm," *Opt. Express*, vol. 18, no. 22, pp. 22928–22936, Oct. 2010.

[17] C. A. Morton, C. Whitehurst, J. V. Moore, and R. M. Mackie, "Comparison of red and green light in the treatment of Bowen's disease by photodynamic therapy," *Brit. J. Dermatol.*, vol. 143, no. 4, pp. 767–772, Oct. 2000.

[18] E. S. Marmur, C. D. Schmults, and D. J. Goldberg, "A review of laser and photodynamic therapy for the treatment of nonmelanoma skin cancer," *Dermatol. Surg.*, vol. 30, no. 2, pp. 264–71, Feb. 2004.

[19] A. A. Kaminskii *et al.*, "Tetragonal vanadates YVO_4 and $GdVO_4$—New efficient $\chi^{(3)}$-materials for Raman lasers," *Opt. Commun.*, vol. 194, no. 1, pp. 201–206, Jul. 2001.

[20] H. Shen *et al.*, "Simultaneous dual-wavelength operation of Nd-doped yttrium orthovanadate self-Raman laser at 1175 nm and undoped gadolinium orthovanadate Raman laser at 1174 nm," *Appl. Phys. Express*, vol. 6, no. 4, Apr. 2013, Art. no. 042704.

[21] G. Shayeganrad, "Actively Q-switched Nd:YVO_4 dual-wavelength stimulated Raman laser at 1178.9 nm and 1199.9 nm," *Opt. Commun.*, vol. 292, pp. 131–134, Apr. 2013.

[22] H. Shen *et al.*, "Simultaneous dual-wavelength operation of Nd:YVO_4 self-Raman laser at 1524 nm and undoped $GdVO_4$ Raman laser at 1522 nm," *Opt. Lett.*, vol. 37, no. 19, pp. 4113–4115, Oct. 2012.

[23] H. Zhu *et al.*, "Cascaded self-Raman laser emitting around 1.2–1.3 μm based on a c-cut Nd:YVO_4 crystal," *IEEE Photon. J.*, vol. 9, no. 2, Apr. 2017, Art. no. 1500807.

[24] J. J. Zayhowski, "Passively Q-switched Nd:YAG microchip lasers and applications," *J. Alloys Compd.*, vol. 303–304, pp. 393–400, May 2000.

[25] M. A. Albota *et al.*, "Three-dimensional imaging laser radar with a photon-counting avalanche photodiode array and microchip laser," *Appl. Opt.*, vol. 41, no. 36, pp. 7671–7678, Dec. 2002.

[26] A. Agnesi, F. Pirzio, G. Reali, and G. Piccinno, "Subnanosecond diode-pumped passively Q-switched Nd:$GdVO_4$ laser with peak power > 1 MW," *Appl. Phys. Lett.*, vol. 89, no. 10, Jul. 2006, Art. no. 101120.

Authorized licensed use limited to: Xiamen University. Downloaded on November 11,2020 at 03:33:03 UTC from IEEE Xplore. Restrictions apply.

[27] A. C. Butler, D. J. Spence, and D. W. Coutts, "Scaling Q-switched microchip lasers for shortest pulses," *Appl. Phys. B, Lasers Opt.*, vol. 109, no. 1, pp. 81–88, Oct. 2012.
[28] J. J. Zayhowski and A. Mooradian, "Single-frequency microchip Nd lasers," *Opt. Lett.*, vol. 14, no. 1, pp. 24–26, Jan. 1989.
[29] T. Taira, "Domain-controlled laser ceramics toward giant micro-photonics [Invited]," *Opt. Mater. Express*, vol. 1, no. 5, pp. 1040–1050, Sep. 2011.
[30] J. J. Zayhowski, "Microchip lasers," *Opt. Mater.*, vol. 11, nos. 2–3, pp. 255–267, Jan. 1999.
[31] A. A. Demidovich *et al.*, "Sub-nanosecond microchip laser with intracavity Raman conversion," *Appl. Phys. B, Lasers Opt.*, vol. 76, no. 5, pp. 509–514, May 2003.
[32] J. Dong, M. Bass, Y. Mao, P. Deng, and F. Gan, "Dependence of the Yb^{3+} emission cross section and lifetime on temperature and concentration in yttrium aluminum garnet," *J. Opt. Soc. Amer. B*, vol. 20, no. 9, pp. 1975–1979, Sep. 2003.
[33] J. Dong *et al.*, "Composite Yb:YAG/Cr^{4+}:YAG ceramics picosecond microchip lasers," *Opt. Express*, vol. 15, no. 22, pp. 14516–14523, Oct. 2007.
[34] P. Loiko *et al.*, "Sub-nanosecond Yb:$KLu(WO_4)_2$ microchip laser," *Opt. Lett.*, vol. 41, no. 11, pp. 2620–2623, Jun. 2016.
[35] A. A. Lagatsky, A. Abdolvand, and N. V. Kuleshov, "Passive Q switching and self-frequency Raman conversion in a diode-pumped Yb:$KGd(WO_4)_2$ laser," *Opt. Lett.*, vol. 25, no. 9, pp. 616–618, May 2000.
[36] V. E. Kisel, V. G. Shcherbitsky, and N. V. Kuleshov, "Efficient self-frequency Raman conversion in a passively Q-switched diode-pumped Yb:$KGd(WO_4)_2$ laser," in *Proc. Adv. Solid-State Photon.*, 2003, pp. 189–192.
[37] A. S. Grabtchikov *et al.*, "Laser operation and Raman self-frequency conversion in Yb:KYW microchip laser," *Appl. Phys. B, Lasers Opt.*, vol. 75, no. 6, pp. 795–797, Nov. 2002.
[38] J. Liu *et al.*, "Efficient continuous-wave and Q-switched operation of a diode-pumped Yb:$KLu(WO_4)_2$ laser with self-Raman conversion," *Opt. Lett.*, vol. 30, no. 18, pp. 2427–2429, Sep. 2005.
[39] P. Loiko *et al.*, "Passive Q-switching and self-Raman conversion in Yb:$KLu(WO_4)_2$ microchip laser," in *Proc. Eur. Conf. Lasers Electro-Opt.*, 2015, Paper CA_5b_3.
[40] V. E. Kisel *et al.*, "Q-switched Yb^{3+}:YVO_4 laser with Raman self-conversion," *Appl. Phys. B, Lasers Opt.*, vol. 80, no. 4, pp. 471–473, Apr. 2005.
[41] W. Jiang *et al.*, "Q-Switched Yb:YAG/YVO_4 Raman laser," *IEEE Photon. Technol. Lett.*, vol. 27, no. 10, pp. 1080–1083, Mar. 2015.
[42] W. Jiang *et al.*, "YVO_4 Raman laser pumped by a passively Q-switched Yb:YAG laser," *Opt. Express*, vol. 25, no. 13, pp. 14033–14042, Jun. 2017.
[43] P. G. Zverev, "The influence of temperature on Raman modes in YVO_4 and $GdVO_4$ crystals," *J. Phys., Conf. Ser.*, vol. 92, no. 1, 2007, Art. no. 012073.
[44] J. Dong, A. Shirakawa, and K. Ueda, "Switchable pulses generation in passively Q-switched multi longitudinal-mode microchip laser," *Laser Phys. Lett.*, vol. 4, no. 2, pp. 109–116, Feb. 2007.
[45] J. J. Zayhowski and C. Dill, "Diode-pumped passively Q-switched picosecond microchip lasers," *Opt. Lett.*, vol. 19, no. 18, pp. 1427–1429, Sep. 1994.
[46] M. Tsunekane and T. Taira, "Temperature and polarization dependences of Cr:YAG transmission for passive Q-switching," in *Proc. Conf. Lasers Electro-Opt./Int. Quantum Electron. Conf.*, Baltimore, MD, USA, 2009, Paper JTuD8.
[47] H. M. Pask, "Continuous-wave, all-solid-state, intracavity Raman laser," *Opt. Lett.*, vol. 30, no. 18, pp. 2454–2456, Sep. 2005.

Xiao-Lei Wang was born in Shandong, China, in 1988. He received the B.S. degree in electronic information science and technology from Inner Mongolia University of Technology, Hohhot, China, in 2012, and the M.S. degree in optical engineering from Beijing University of Technology, Beijing, China, in 2015. He is currently working toward the Ph.D. degree in physics electronics at Xiamen University, Xiamen, China. His research interests include passively Q-switched microchip lasers and Raman lasers.

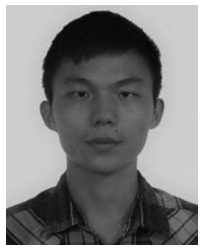

Xiao-Jie Wang was born in Fujian, China, in 1991. He received the B.S. degree in communication engineering from the Huaqiao University, Xiamen, China, in 2015. He is currently working toward the Master's degree in electronics and communication engineering at Xiamen University, Xiamen, China. His research interests include passively Q-switched microchip lasers and Raman lasers.

Jun Dong (M'10) received the B.S. and M.S. degrees in material science from Xi'an Jiaotong University, Xi'an, China, in 1992 and 1997, respectively, and the Ph.D. degree from Shanghai Institute of Optics and Fine Mechanics, Chinese Academy of Sciences, Shanghai, China, in 2000.

He was a Research Scientist with the Optical Material Research Center, Shanghai Institute of Optics and Fine Mechanics, Chinese Academy of Sciences, from 2000 to 2001. He also was a Research Scientist with the School of Optics/CREOL/FPCE, University of Central Florida, Orlando, FL, from 2001 to 2003. From 2003 to 2007, he was a Research Fellow with the Institute for Laser Science, University of Electro-Communications, Tokyo, Japan. From 2007 to 2008, he was a Research Associate with the School of Engineering and Physical Sciences, Heriot-Watt University, Edinburgh, U.K. He has been a Professor with the Department of Electronic Engineering, School of Information Sciences and Technology, Xiamen University, Xiamen, China, since 2008. He has authored or co-authored more than 120 scientific publications. His research interests include the fabrication and fundamental investigation of transparent laser ceramics, ceramic lasers, laser diode pumped solid-state lasers and amplifiers, especially passively Q-switched Yb- and Nd-doped crystals and ceramics lasers using Cr^{4+}-doped materials as saturable absorber, and second-harmonic generation in these lasers, and mechanical properties and optical properties of the laser materials.

Dr. Dong is a Senior Member of the Optical Society of America.

Authorized licensed use limited to: Xiamen University. Downloaded on November 11,2020 at 03:33:03 UTC from IEEE Xplore. Restrictions apply.